Proceedings of the 7th IEEE
International Conference on Nanotechnology
August 2 - 5, 2007, Hong Kong

Image-Based Hysteresis Modeling and Compensation for Piezo-Scanner Utilized in AFM

Yudong Zhang, Yongchun Fang*, *IEEE, Member*, Xianwei Zhou, and Xiaokun Dong

Institute of Robotics and Automatic Information System, Nankai University, China

***Abstract* — As an important component of Atomic Force Microscope (AFM), piezo-scanner exhibits some undesired nonlinear characteristics, among which the inherent hysteresis largely decreases the scanning rate and resolution of AFM. To alleviate this problem, an image-based approach is proposed in this paper to model and then compensate for the hysteresis behavior of the piezo-scanner. Specifically, some scanning images over calibration grating are utilized to identify the parameters of the classical Preisach model (CPM) of hysteresis. Based on the obtained model, an inversion-based technique is adopted to design a compensator for the hysteresis of piezo-scanner. The proposed algorithm presents such advantages of low cost and little complexity since no nano-sensor is required to collect identification data. Some simulation results are included to demonstrate the performance of the proposed strategy.**

Keywords — Atomic Force Microscope(AFM); Piezo-Scanner; Hysteresis; Image; Compensation

I. INTRODUCTION

In the field of nanotechnology, atomic force microscope is a fundamental instrument, and it plays an important role in nano-imaging, nano-manipulating, and so on. The 3-dimentional piezo-scanner is usually employed in AFM system to generate fine displacements, including x, y lateral periodical trajectory for scanning process, desired trajectory for nano-manipulating, and z-displacement for constant force control. It has many advantages, such as high resolution, fast frequency response, and high stiffness. However, piezo-scanner exhibits some undesired nonlinear characteristics, such as hysteresis, structural dynamics, and creep. These drawbacks increase the difficulty of achieving images of high resolution. Subsequently, the scanning operation has to be done under low frequency, which then hinders the wide application of AFM system.

Many researches have been devoted to model and compensate for hysteresis characteristics of piezo-scanner. According to the modeling mechanism, there are two types of model describing the hysteresis behavior. The first type is called constitutive model which has explicit physical meaning, such as Jiles-Atherton model ([1] offers a numerical implementation of J-A model) and homogenized energy model [2], but many involved parameters need to be identified and they are usually sensitive to exotic environment. Therefore, these models are not frequently employed in practical systems. The other type is often referred to as phenomenological model, which is actually a mathematical approximation for the hysteresis nonlinearity. Among these models, Duhem model [3], Bouc-Wen model [4] and friction model are all based on the nonlinear differential equation which facilitates the design of feedback controller. In contrary to them, classical Preisach model (CPM) [5] based on integral is the mostly used one as it can approach to the actual values infinitely and its inversion can be obtained easily. To simplify the computation task, some models similar to CPM have also been exploited in practice, such as P-I model [6] and K-P model. Recently, with the development of intelligent algorithms, many efforts have been made to model hysteresis using neural network [7].

To weaken the hysteresis nonlinearity, both open loop and closed loop control methods have been reported to achieve desired performance. Charge actuating is a typical model-free feed-forward control method which mainly depends on the designs of the hardware. Besides, the inversion of the aforementioned mathematical models is employed as feed-forward section to compensate for hysteresis of piezo-scanner. Unfortunately, open loop control strategy often exhibits such disadvantages as poor robustness over various disturbances, and it usually cannot achieve the desired position precision. Therefore, many closed-loop control techniques have recently been implemented for AFM system based on the analysis of the hysteresis dynamics, such as the classical proportion-integral-derivative (PID) control, adaptive control and robust H_∞ control. However, in these systems, some nano-sensors, including linear variable differential transformer (LVDT), laser interferometer, and capacitance sensor, are required to obtain measurement for feedback.

More recently, some of the aforementioned control methods have been successfully implemented to the piezo-scanner utilized in AFM to increase its measurement/manipulation performance. In [8], a new dc accurate charge amplifier was shown to significantly reduce hysteresis while avoiding characteristic voltage drift simultaneously. In [9], a compensator was designed to reduce the hysteresis behavior of piezo-scanner. In [10], by utilizing CPM model, *Ying Wu* proposed an inversion-based iterative controller to obtain a better performance of AFM system. In [2], based on the analysis of the homogenized energy model, an inverse filter was constructed to attenuate hysteresis and finally obtained a roughly linear input-output behavior for ferroelectric transducers.

Unfortunately, to identify the model parameters, all of the aforementioned methods of piezo-scanner require a nano-sensor to measure the actual displacement of piezo-scanner. However, it is usually difficult and costly in practice to equip commercial AFM with nano-sensor on piezo-scanner. Motivated by this fact, an image-based approach is proposed in this paper to model and then compensate for the hysteresis

This project was funded by the National Natural Science Foundation of China (Project code: 60574027)
**Contact author: yfang@robot.nankai.edu.cn*

of the piezo-scanner without the utilization of nano-sensor. Specifically, in this research, the CPM is chosen as the model for hysteresis due to its high accuracy, and an image-based approach is then designed to identify system parameters. Consequently, based on the inversion of the obtained CPM model, a compensator is proposed to attenuate the hysteresis behavior. Compared with conventional methods, the proposed image-based modeling strategy involves no expensive nano-sensor, and it is easier to implement in practice. Simulation results demonstrate that the obtained model accurately describes the hysteresis nonlinearity and the compensator effectively improves the performance of AFM.

The rest of the paper is organized as follows. Section II gives a brief introduction for the CPM model, and then explains the image-based parameter identification method in detail. In section III the recursive implementation of CPM model is presented and an inversion-based compensator is then constructed. Simulation results of scanning calibration grating are provided in section IV to illustrate the effectiveness of the proposed strategy. Finally, section V summarizes this paper and gives some plans for future work.

II. IMAGE-BASED HYSTERESIS MODELING

A. Classical Preisach Model

CPM can be regarded as the superposition of series of hysteresis operators called hysteron, as depicted in Figure 1. (a), in which the play-stop operator is often utilized with output as 0 or 1.

Define $v = \gamma_{\alpha\beta}[u(t)]$ as the output of the hysteron, and let $\zeta \in \{0,1\}$, $t \in (0,T]$, then the hysteresis operator can be described as:

$$v(0) \triangleq \begin{cases} 0 & u(0) \le \beta \\ \zeta & \beta < u(0) < \alpha \\ 1 & u(0) \ge \alpha \end{cases} \quad (1)$$

Assume that $X_t \triangleq \{\tau \in (0,t] : u(\tau) = \beta \text{ or } \alpha\}$, then the output of this operator during $t \in (0,T]$ can be obtained as follows:

$$v(t) \triangleq \begin{cases} v(0) & \text{if } X_t = \varnothing \\ 0 & \text{if } X_t \neq \varnothing \text{ and } u(\max X_t) = \beta \\ 1 & \text{if } X_t \neq \varnothing \text{ and } u(\max X_t) = \alpha \end{cases} \quad (2)$$

The CPM model can be described as the double integral of the triangle area (see Figure 1. (b)) in which every point represents a hysteron, and for each hysteron, there exists a corresponding weight $\mu(\alpha,\beta)$:

$$f^P(t) = H[u(t)] = \iint_{\alpha \ge \beta} \mu(\alpha,\beta)\gamma_{\alpha\beta}[u(t)]d\alpha d\beta \quad (3)$$

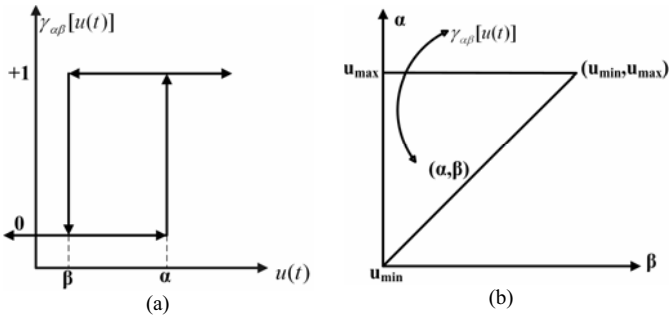

Figure 1. (a) The play-stop Preisach operator, values {0, 1}; (b) Preisach plane

where $f^P(t)$ is the output of the CPM, and $\gamma_{\alpha\beta}[u(t)]$ stands for the output of the Preisach operator.

Note that the value of $\gamma_{\alpha\beta}[u(t)]$ not only lies on the current input $u(t)$, but also relates to the previous input, therefore the CPM model can capture the hysteresis characteristic remarkably.

B. Image-Based Parameters Identification

The key issue of modeling hysteresis is to determine the weights of the integral plane. From (3), it can be seen that the twice differentials have to be calculated in order to obtain these weights, which then leads to large error because the noise is often amplified by the differential operation. A discrete recursive method, which is easy to implement in computer, is designed to avoid this problem. When identifying these weights, the mostly utilized method is called first order reversal functions (FORF) [5] which employs a nano-sensor (such as LVDT, capacitance sensor) for measurement and requires strict initial conditions. Hence, this method is not suitable for the modeling of the piezo-scanner utilized in AFM as it is apparently difficult and costly to design and fixes a nano-sensor on the scanner. In this paper, considering the periodicity of the actuating signal and the congruency property of CPM (see Figure 2.), the scanned image data is employed to determine the weights without utilization of any nano-sensor.

To collect experimental data, the input exerted on the piezo-scanner of AFM ranges from -160V to 160V, and it is evenly divided into 32 sub-ranges to obtain a discrete integral plane as Figure 3. Image data is then obtained by scanning the sample of calibration grating to identify the weights corresponding with each hysteron of the integral plane.

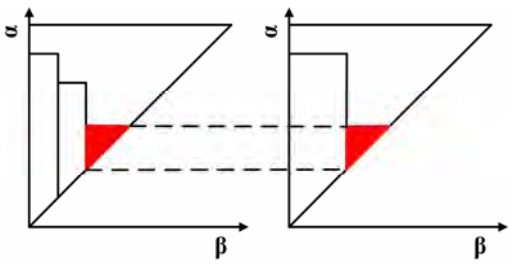

Figure 2. Congruency property, the integral values of the red triangle in the two integral planes is equivalent whereas the previous input may be different.

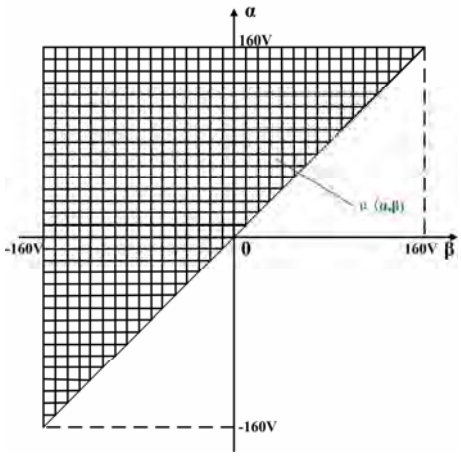

Figure 3. Discrete Preisach plane, minimum of u is -160v, maximum of u is 160V, space is 10V.

Specifically, a one dimension calibration grating with a nominal period of 278nm is utilized as the standard sample for scanning. In practice, the period may be changed as the sample orientation has to be determined after analyzing a full image. To collect data, the calibration grating is scanned with 16ranges, from [-160V, 160V] to [-10V, 10V] by bi-direction manner. The scan is performed under a comparatively low frequency so that the dynamics of AFM can be ignored.

The gravity center method is then applied on the obtained image to extract the feature points, which stand for the peak points of the grating, as depicted by the red circles in Figure 4. Specifically, the following formula is utilized to set the threshold:

$$h = \frac{\sum_{i=1}^{n} height(i)}{n} a + c \tag{4}$$

where n is the number of scanned pixels, c and a are some parameters which can be set to avoid the small noise created during scanning, $height(i)$ represents the height information of the ith point. Then the pixels of feature points can be obtained as follows:

$$p = \frac{\sum_{i=m}^{n} (pixel(i) * height(i))}{\sum_{i=m}^{n} height(i)} \tag{5}$$

where $height(i)$ is the height of sample surface at pixel i, and it is larger than the threshold calculated by (4) for all $i \in [m,n]$.

Since the obtained two adjacent feature points correspond with two neighboring peak points of the grating, their distance then equals the period of the calibration grating, and it should be invariant with different adjacent points if the calibration grating is completely periodic. Based on this fact, the

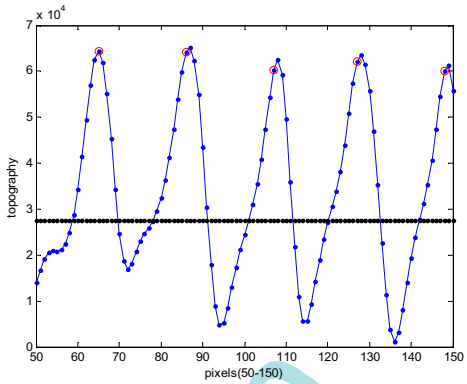

Figure 4. Feature points obtained via gravity center method, where the red circles are the feature points, and the black line is the chosen threshold.

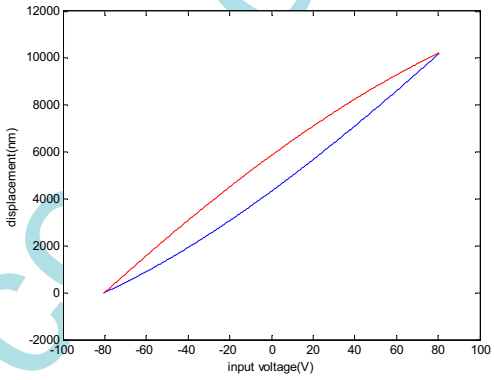

Figure 5. Approximation curves from least square method

displacements of piezo-scanner can be obtained by counting the number of feature points, while the input voltage is directly obtained through the pixels multiplying the space voltage. Then, the input-output map is approximated by a polynomial curve (see Figure 5.) through the least square method (LS):

$$\hat{\theta} = (\Phi_N{}^T \Phi_N)^{-1} \Phi_N{}^T y_N \tag{6}$$

where $\hat{\theta}$ is the parameters of the polynomial curve, Φ_N is the input voltage matrix, and y_N is the output vector.

For each scanning range, the relative displacements of integral curve vertexes are computed through a similar polynomial curve approximation. Then the weight of every block in the discrete integral plane is calculated recursively (see Figure 6. for details).

III. INVERSION-BASED COMPENSATION

A. Recursive Implementation of CPM

The weights of the discrete integral plane can be obtained based on the scanned image data. However, the actual input of piezo-scanner is continuous, a recursive implementation of CPM is introduced based on the FORF method in order to obtain a continuous inversion of the CPM [5].

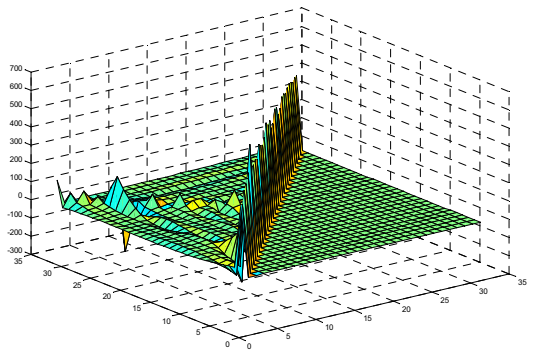

Figure 6. Three dimensional graphics of weights for the piezo-scanner utilized in AFM (Benyuan CSPM 4000, P. R. China)

As depicted in Figure 7. (a), f_α stands for the displacement of piezoceramic when the input ascends from $u_{\min}$ to α, while $f_{\alpha\beta}$ stands for the displacement of piezoceramic when the input descends to β after ascending from $u_{\min}$ to α. The functions f_α and $f_{\alpha\beta}$ are called first order reversal functions. We can easily get the values of f_α and $f_{\alpha\beta}$ when α and β are vertex of the integral plane as the weight of each block in Figure 3. is available. For any other values of α and β, the interpolation method is usually used to calculate f_α and $f_{\alpha\beta}$:

$$f_{\alpha\beta} = c_0^{\alpha\beta} + c_1^{\alpha\beta}\alpha + c_2^{\alpha\beta}\beta + c_3^{\alpha\beta}\alpha\beta \tag{7}$$

where the coefficients (c_0, c_1, c_2, c_3) are obtained by solving the equation group which is formed by substituting the four FORF values into it, such as the example shown in the red circle in Figure 7. (b). Note that only three FORF values are substituted into (7) for the triangle while $c_3^{\alpha\beta}$ is set to zero.

As the first order reversal functions can be computed by (7) for any α and β, the output corresponding to $u(t_n)$ can be expressed as:

$$f^p(t_n) = f^p(t_m) + f_{u(t_n)} - f_{u(t_n)u(t_m)} \tag{8}$$

where $f^p(t_n)$ is the displacement at t_n, $f^p(t_m)$ is the absolute displacement of piezo-scanner at the starting voltage.

B. Inversion-based Compensation of Hysteresis

In this section, based on the recursive implementation of CPM, an inversion of CPM is constructed to compensate for the nonlinearity of hysteresis. As depicted in Figure 8. , the tracking signal $r(t)$, together with the obtained CPM model, is utilized to calculate a suitable input $u(t)$ into the piezo-scanner to achieve the desired performance.

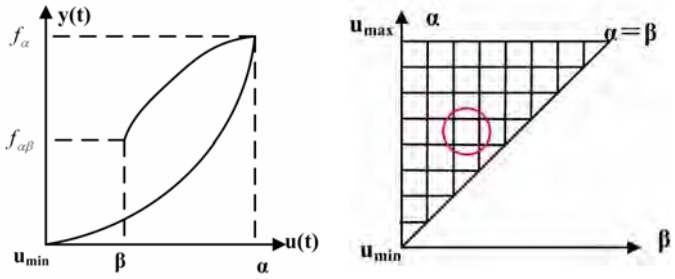

(a) (b)

Figure 7. (a) shows the first order reversal function; (b) shows the interpolation process

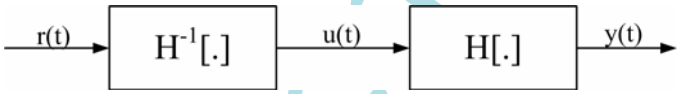

Figure 8. Compensation framework

Substituting (7) into (8) introduced in last section, it can be expressed as:

$$f^P(t_n) = f^P(t_m) + c_0^{u(t_n)} + c_1^{u(t_n)}u(t_n) + c_2^{u(t_n)}u(t_n) - (c_0^{u(t_n)u(t_m)} + c_1^{u(t_n)u(t_m)}u(t_n) + c_2^{u(t_n)u(t_m)}u(t_m) + c_3^{u(t_n)u(t_m)}u(t_n)u(t_m)) \tag{9}$$

After some arrangement, we obtain:

$$f^P(t_n) = f^P(t_m) + c_0^{u(t_n)} - c_0^{u(t_n)u(t_m)} - c_2^{u(t_n)u(t_m)}u(t_m) + (c_1^{u(t_n)} + c_2^{u(t_n)} - c_1^{u(t_n)u(t_m)} - c_3^{u(t_n)u(t_m)}u(t_m))u(t_n) \tag{10}$$

Then, the desired input voltage can be easily obtained as:

$$u(t_n) = \frac{f^P(t_n) - f^P(t_m) - (c_0^{u(t_n)} - c_0^{u(t_n)u(t_m)} - c_2^{u(t_n)u(t_m)}u(t_m))}{c_1^{u(t_n)} + c_2^{u(t_n)} - c_1^{u(t_n)u(t_m)} - c_3^{u(t_n)u(t_m)}u(t_m)} \tag{11}$$

Now, the remaining problem is to determine these coefficients appeared in (11). The following procedures are adopted to calculate the input after compensation:

(1) Set $u(t_n) = u(t_{n-1})$ to obtain a group of coefficients;

(2) Substitute these coefficients into equation (11), if the acquired $u(t_n)$ and the one set previously are in the same block of integral plane (Figure 3.), it implies that these coefficients are valid, and the calculated $u(t_n)$ is the desired input at t_n, then the process stops; otherwise, these coefficients are still incorrect, thus go to (3) to reset them;

(3) As the input is monotonically increasing, set $u(t_n) = u(t_n) + 10V$, where $10V$ is the space of the integral plane, then go to (2) to update the group of coefficients.

The inversion-based compensation algorithm described above is utilized for the duration when the actuating voltage is ascending. After following the same process, the compensation strategy for descending input can be similarly obtained based

on the expressions of (9) and (11). Hence, the triangle trajectory for bi-directional scanning and random trajectory for nano-manipulation can be compensated exactly.

For every desired scanning scope, the compensation work is done as the following steps. Firstly, the input range is computed using recurrence method. Secondly, based on the inverse compensation, an input sequence which amounts to the desired pixels is calculated. Then apply this input sequence to the piezo-scanner and execute the scan process, a high quality scanning image can be achieved.

As the proposed compensation algorithm successfully addresses the hysteresis of piezo-scanner for any desired trajectory, the bi-directional scanning can be possibly achieved by applying this technology to the AFM system, while most current AFM offers only one direction scan due to the hysteresis nonlinearity. In general, this research work will not only enhance the scan accuracy, but it is also possible to speed up the scanning rate and reduce the damage to the sample simultaneously.

IV. SIMULATION RESULTS

In this simulation, the model identified in section II is employed as the hysteresis model of piezo-scanner in x-axis (in this paper, we only presents the analysis for x-axis, the model of y-axis can also be obtained in the same way), and a 5th order linear system model identified by 4SID is used as the AFM z-axis model [11]:

$$G(z)=\frac{-0.00011z^4+0.001512z^3+0.01062z^2+0.01057z-0.0008574}{z^5-0.9979z^4-0.6761z^3+0.6541z^2+0.5269z-0.3975} \quad (12)$$

In order to evaluate the efficiency of the proposed compensation strategy, a calibration grating with a period of 278nm is chosen as the sample. And the scanning scope and resolution are set as 3000nm and 512*512 respectively. In z-axis, the classical PID control method is utilized to keep the output constant. Figure 9. shows the simulation results with and without compensation under the same frequency of 5Hz (five lines per second). It can be seen that the result without compensation (see Figure 9. (a)) distorts image sharply, and it destroys the periodic characteristics of the grating. In contrast, as shown in Figure 9. (b), the inversion-based compensation algorithm effectively attenuates the hysteresis of piezo-scanner, and the scanned image reflects the actual topography of the grating accurately.

V. CONCLUSIONS

In summary, this paper proposes an image-based method to model the characteristics of hysteresis existing in the piezo-scanner, then based on the obtained model, a numerical recursive inversion-based compensator is designed to largely eliminate the effect of hysteresis. Simulation results are provided to show that high quality image can be obtained for samples after this compensation of hysteresis. Besides, due to the attenuation of hysteresis, bidirectional scanning can be possibly achieved which subsequently enhances the scanning speed and resolution of the AFM system. Moreover, it is

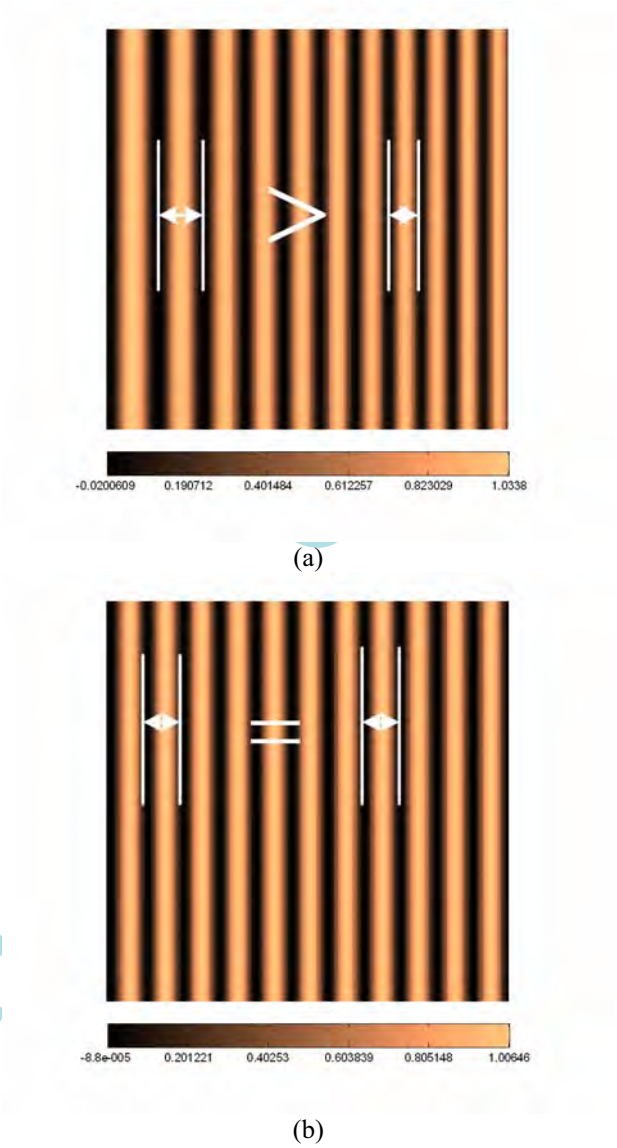

Figure 9. Simulation results of the scanning over a periodic calibration grating (a) Without hysteresis compensation. (b) With compensation for hysteresis.

believed that the compensation work will improve the nano-positioning accuracy during nano-manipulation.

As the image data for modeling is acquired under low frequency, the feed-forward control based on the inversion of the static Preisach model can only be implemented with slow scanning speed. Therefore, this method mainly improves the imaging accuracy under low frequency. Besides, the effect of creep is not considered strictly in this research, however, it will influence the performance when working with a long time. Therefore, future work will study the dynamics of piezo-scanner, together with the hysteresis described by the static Preisach model. Consequently, the Hammerstein model will be employed to describe the full nonlinearity of piezoceramic. And based on this model, some modern control strategies will be developed to enhance both the scanning resolution and speed.

ACKNOWLEDGMENT

The authors thank the support from Being Nano-Instruments Ltd. for their heartful help.

REFERENCES

[1] Dieter Lederer, Hajime Igarashi, Arnulf Kost and Toshihisa Honma, "On the Parameter Identification and Application of the Jiles-Atherton Hysteresis Model for Numerical Modelling of Measured Characteristics", *IEEE Trans. Magnetics*, Vol. 35, No. 3, pp. 1211-1214, May 1999.

[2] Andrew G. Hatch, Ralch C. Smith, Tathagata De, and Murti V. Salapaka, "Construction and Experimental Implementation of a model-Based Inverse Filter to Attenuate Hysteresis in Ferroelectric Transducers", *IEEE Trans. Control Systems Technology*, Vol. 14, No. 6, pp.1058-1069, Nov. 2006.

[3] JinHyoung Oh, Dennis S. Bernstein, "Semilinear Duhem Model for Rate-Independent and Rate-Dependent Hysteresis", *IEEE Trans. Automatic Control*, Vol. 50, No. 5, pp. 631-645, May 2005.

[4] Fayçal Ikhouane, Víctor Mañosa, José Rodellar, "Dynamic properties of the hysteresis bouc-Wen model", *Systems & Control Letters*, 56(2007), pp. 197-205.

[5] Hong Hu, "Compensation of Hysteresis in Piezoceramic actuators and Control of Nanopositioning System", *Ph. D Disseration*, Dept. Mechnical and Industrial Engineering, University of Toronto, 2003.

[6] Wei Tech Ang, Francisco Alija Garmón, Pradeep K. Khosla, and Cameron N. Riviere, "Modeling Rate-dependent Hysteresis in Piezoelectric Actuators", *Proc. of the 2003 IEEE/RSJ Intl. Conf. on Intellient Robots and Systems*, Las Vegas, Nevada, pp. 1975-1980, Oct. 2003.

[7] Li Chuntao, Tan Yonghong, "A Neural Networks Model for Hysteresis Nonlinearity", *Sensors and Actuators*, A 112, 2004, pp. 49-54.

[8] Andrew J. Fleming, S. O. Reza Moheimani, "Sensorless Vibration Suppression and Scan Compensation for Piezoelectric tube Nanopositioners", *IEEE Trans. Cont. Syst. Tech*, Vol. 14, No. 1, pp. 33-44, Jan. 2006.

[9] D. Croft, G. Shedd, and S. Devasia, "Creep, Hysteresis, and Vibration Compensation for Piezoactuators: Atomic Force Microscopy Application", in *Proc. 2000 American Control Conference*, Chicago, Illinois, pp.2123-2128, June, 2000.

[10] Ying Wu and Qingze Zou, "Iterative Control Approach to Compensate for the Hysteresis and Vibrational Dynamics Effects of Piezo Actuators" in *Proc. 2006 American Control Conference*, Minneapolis, USA, 2006, pp. 424-429.

[11] Xianwei Zhou, Yongchun Fang, Xiaokun Dong, Yudong Zhang, "System Modeling of an AFM System in Z-axis", I*EEE –NANO*, 2007, Hong Kong, China, Accepted.